Journal of Sea Research 75 (2013) 96–109

Contents lists available at SciVerse ScienceDirect

Journal of Sea Research

journal homepage: www.elsevier.com/locate/seares

Combining field observations and modeling approaches to examine Greenland halibut (*Reinhardtius hippoglossoides*) early life ecology in the southeastern Bering Sea

J.T. Duffy-Anderson [a,*], D.M. Blood [a], W. Cheng [b], L. Ciannelli [c], A.C. Matarese [a], D. Sohn [c], T.C. Vance [a], C. Vestfals [c]

[a] Recruitment Processes Program, Resource Assessment and Conservation Engineering Division, Alaska Fisheries Science Center, NOAA Fisheries, 7600 Sand Point Way NE, Seattle, WA 98115, USA
[b] Joint Institute for the Study of the Atmosphere and Ocean, P.O. Box 354235, University of Washington, Seattle, WA 98195, USA
[c] College of Oceanic and Atmospheric Sciences, Oregon State University, Corvallis, OR 97331, USA

ARTICLE INFO

Article history:
Received 2 November 2011
Received in revised form 21 June 2012
Accepted 29 June 2012
Available online 13 July 2012

Keywords:
Greenland halibut
Larvae
Transport
Bering Sea
Connectivity

ABSTRACT

Spawning in Greenland halibut (*Reinhardtius hippoglossoides*) occurs along the continental slope and in submarine canyons in the eastern Bering Sea. It is assumed that these bathymetric features and their associated circulation patterns deliver eggs and larvae to suitable nursery habitats over the continental shelf. However, there have been no directed field studies examining spawning areas or transport of Greenland halibut early life stages in the Bering Sea, nor is it known how large-scale oceanographic forcing modulates specific physical mechanisms of delivery. The present study was undertaken to: better define spawning areas of Greenland halibut, examine development and distribution of larvae, and understand the influence of climate variations on interannual patterns of transport, distribution and abundance. Eggs were found in Bering and Pribilof Canyons and over the adjacent slope in February and early March, confirming that spawning occurs in these regions. Larvae were present over the slope, outer shelf and middle shelf in winter and spring, and settled juveniles were collected over the shelf in September. Oceanographic modeling approaches that simulate larval advection from spawning to nursery habitats indicate that depth-discrete variations in transport pathways from submarine canyons to the adjacent shelf contribute to interannual variability in transport trajectories. Overall, our results highlight specific physical mechanisms of delivery that are modulated by large-scale atmospheric and oceanographic forcing, potentially varying the degree of slope–shelf connectivity for Greenland halibut and other slope-spawning species.

Published by Elsevier B.V.

1. Introduction

The role of oceanographic features in structuring marine habitat use has long been an area of intense scientific interest and research effort. Fundamental theories espouse that on evolutionary time scales, fishes spawn in areas with existing bathymetric features and persistent circulation patterns that deliver larvae to suitable nursery habitats. Deep water (>400 m), slope-spawning species that have juveniles that recruit to nursery habitats over the continental shelf (<200 m) must contend with the necessity of spawning in areas that afford vertical connectivity in addition to horizontal connectivity. For these species, propagules must be reliably advected up the slope margin and then across the continental shelf to target nursery habitats. Deepwater flatfishes are particularly well-adapted to this unique combination of criteria (e.g., Bailey et al., 2008; Minami and Tanaka, 1992). However, though species may be well-adapted to make use of environmental features that promote directed transport of offspring, it is likely that the specific physical mechanisms of delivery are modulated by large-scale atmospheric and oceanographic forcing, potentially varying the degree of slope–shelf connectivity.

The southeastern Bering Sea (Fig. 1) is characterized by a deep basin (depth range 200–3500 m) and a wide continental shelf (>500 km) which is further subdivided by bathymetry into three major domains: the inner continental shelf (<50 m), the middle shelf (50 m–100 m), and the outer shelf (100 m–200 m). General circulation in the basin is in the form of a cyclonic gyre, with the Kamchatka Current forming the western boundary, the Aleutian North Slope Current flowing eastward along the Aleutian Islands, and the Bering Slope Current forming the eastern boundary (Stabeno et al., 1999). Several submarine canyons traverse the slope margin, Zhemchug Canyon to the north, followed by Pribilof, and Bering Canyons to the south (Fig. 1). Pribilof and Zhemchug Canyons have trough shaped basins while Bering Canyon has a wide slope valley (>400 km). These canyons and adjacent slopes form important spawning grounds for a number of marine fish and elasmobranch species including skates (Hoff, 2010), rockfishes (Love et al.,

* Corresponding author. Tel.: +1 11 206 526 6465.
E-mail address: Janet.Duffy-Anderson@noaa.gov (J.T. Duffy-Anderson).

1385-1101/$ – see front matter. Published by Elsevier B.V.
doi:10.1016/j.seares.2012.06.014

2002), smoothtongues (Sinclair and Stabeno, 2002), and flatfishes (Sohn et al., 2010; St-Pierre, 1984), and are hypothesized to facilitate flux of water and entrained particles from the basin to the shelf (Normark and Carlson, 2003).

Spawning in the circumpolar deepwater flatfish, Greenland halibut (*Reinhardtius hippoglossoides*), also known as Greenland turbot (Ianelli et al., 2011), in the Bering Sea is believed to occur over the slope and in large submarine canyons, with larvae and juveniles recruiting to the middle and outer domains of the continental shelf (Sohn et al., 2010). Spawning has generally been inferred from observations of distribution of larval stages, as published reports of egg distributions for this species in the Pacific are few (Bulatov, 1983; Mikawa, 1963; Pertseva-Ostroumova, 1961). The lack of data has been based, in part, from the inability to conclusively identify Greenland halibut eggs based on morphology alone. Moreover, a comprehensive morphological description is lacking for Greenland halibut early life stages collected in the North Pacific, though some information for the species in the North Atlantic has been published (Stene et al., 1999).

Oceanographic modeling has been previously used to examine dispersal and transport pathways of Greenland halibut in Greenland waters and in the north-east arctic (Ådlandsvik, 2000; Ådlandsvik et al., 2004). This approach revealed that transport of Greenland halibut early life stages in these systems is dependent upon spawning location, transport depth, and interannual variability in dominant flow regime. The present study aimed to continue and extend the published work on Greenland halibut to the Bering Sea by: 1) using directed field sampling (2006–2010) to more completely describe early life ecology in Bering Sea, 2) providing a more complete taxonomic description of the morphology and development of the early life stages, and 3) employing an oceanographic circulation model to better understand how climate variations may affect interannual patterns of transport, distribution and connectivity of this species between spawning and nursery areas.

2. Materials and methods

2.1. Study area and biological sampling

The geographic regions of sampling were the eastern Bering Sea (EBS) slope and adjacent shelf in the vicinity of Bering and Pribilof Canyons (Fig. 1). Multiple field surveys (February, May, September) were conducted over a period of four years (2006–2010) aboard the NOAA Ships *Miller Freeman* and *Oscar Dyson* (Table 1). All months were not sampled in all years because cruise timing was opportunistic and occasionally constrained by logistical factors. The primary objective of Greenland halibut work on all cruises was to examine the abundance and distribution of Greenland halibut eggs, larvae, and juveniles in the EBS. Depth-integrated egg and larval samples were collected using 60 cm bongo nets strung with 0.505 mm mesh. Tows were to 10 m off-bottom over the continental shelf, and to 500 m or 600 m over the slope and basin as determined in real time. Vertically stratified tows were conducted at selected stations when eggs were observed in bongo collections. Depth intervals sampled were: 0–20 m, 20–30 m, 30–40 m, 40–50 m, 50–100 m, 100–200 m, 200–300 m, and 300–400 m. Depth-discrete sampling was accomplished using the Multiple Opening and Closing Net and Environmental Sensing System (MOCNESS; Wiebe et al., 1976). The volume of water filtered by both types of nets was estimated using calibrated flow meters. The ship's speed was adjusted to maintain a tow wire angle of 45°. Upon net retrieval, ichthyoplankton samples were immediately preserved in 5% buffered formaldehyde. Preserved samples were sorted and larvae were identified and measured (standard length in mm, SL) at the Plankton Sorting and Identification Center in Szczecin, Poland. Verification of all larval identifications and egg measurements was done at either Oregon State University in Corvallis, OR, USA or at the Alaska Fisheries Science Center (AFSC), in Seattle, WA, USA.

Settled juvenile Greenland halibut were collected in autumn using a 3.05 m plum staff beam trawl rigged with 7 mm mesh, a 4 mm cod end liner, and tickler chains (Gunderson and Ellis, 1986). Towing speeds ranged from 1.5 to 3 knots. The towed area was calculated and data were standardized to CPUE for an area of 1000 m^2. Juvenile Greenland halibut were identified, separated from the main catch, and immediately frozen at −20 °C. In the laboratory, samples were thawed, identifications were verified, and individuals were measured (total length in mm, TL).

2.2. Physical environment

Physical data were collected simultaneously with biological samples using either SeaBird[1] SBE 911 plus Conductivity Temperature Depth (CTD) casts, a SeaBird[1] SEACAT profiler SBE 19 Plus attached in-line with plankton net arrays, or a net-mounted SeaBird[1] SBE-39 temperature and depth profiler attached to the beam trawl (juveniles).

2.3. Egg and larval taxonomy and development

Taxonomic and morphological data were obtained from eggs and larvae collected during the above ichthyoplankton surveys and from historical surveys conducted from 1979 to 2009 by the Recruitment Processes Program at the AFSC.[2]

Marine teleost eggs are typically identified by their size if they are in the early stage of development and the embryo has not formed, or if distinctive characters are not visible from the developing embryo. Conclusive identification of early-stage Greenland halibut eggs in the Bering Sea has been confounded by the presence of Pacific halibut (*Hippoglossus stenolepis*) eggs, which spatially and temporally co-occur with Greenland halibut eggs (Matarese et al., 1989; 2003). Late-stage Greenland halibut eggs can be identified by the 60–65 myomeres visible in the embryo as compared to Pacific halibut that have a maximum of 51 myomeres. To determine whether Greenland halibut eggs could be identified from the Bering Sea, we conducted an extensive examination of historical collections of Pacific halibut eggs collected in the Gulf of Alaska, where Greenland halibut do not occur. We reasoned that if we could determine a maximum size for Pacific halibut eggs from the Gulf of Alaska collections (193 eggs), we could assume that early-stage eggs collected in the Bering Sea that exceeded the maximum size of Pacific halibut eggs were probably Greenland halibut. Using this approach we determined that all Pacific halibut eggs from the Gulf of Alaska were <3.5 mm diameter, and assumed that all eggs ≥ 3.5 mm diameter in the Bering Sea were those of Greenland halibut. The smallest late-stage egg that could be positively identified as Greenland halibut was 3.54 mm, which was close to our threshold size. It should be noted that we do not know the minimum size of Greenland halibut eggs, and eggs smaller than 3.5 mm diameter in our collections may have been erroneously identified as Pacific halibut. Thus our approach may have underestimated abundances of Greenland halibut eggs collected from our surveys, and the values should be considered conservative.

2.4. Egg developmental staging

Greenland halibut eggs were staged according to developmental criteria described by Blood et al. (1994) according to a 21-stage schedule developed and standardized for walleye pollock (*Theragra chalcogramma*). Staging criteria for walleye pollock are the standards to which northern marine teleost egg development are compared and were easily adapted to egg development in Greenland halibut. Eggs

[1] Use of trade name does not imply endorsement by NOAA Fisheries.
[2] http://access.afsc.noaa.gov/ichthyo/index.cfm.

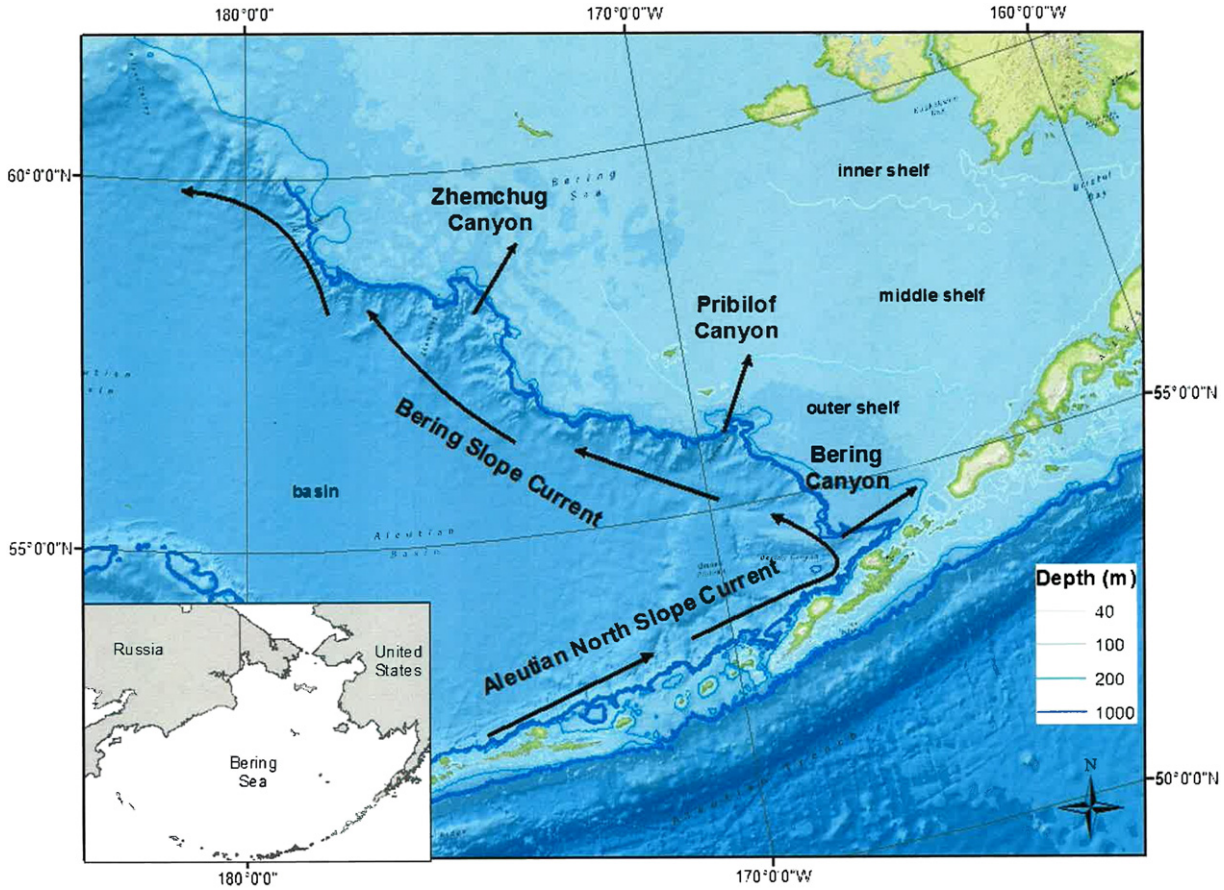

Fig. 1. Study area over the Bering Sea basin, slope, and shelf. Major current pathways were expressed as black arrows.

were then binned into broader categories (Duffy-Anderson et al., 2011) that comprised the Early Stage (stages 1–12), which includes all stages prior to the closing of the blastopore; Middle Stage (stages 13–15), when the blastopore is closed, the margin of the tail is defined, and the tail bud is thick, but the margin remains attached to the yolk; and Late Stage (16–23), when the tail lifts away from yolk, and lengthens and encircles the top half of the yolk to extend just beyond the head of the embryo.

Changes in vertical distribution of eggs by developmental stage were examined from depth-discrete MOCNESS tows. Supplementary depth information was provided from bongo tows by calculating the catch-weighted-mean depth of each egg stage (CWMD) according to:

$$\mathrm{CWMD} = \sum_{i=1}^{n} x_i d_i / \sum_{i=1}^{n} x_i$$

where x_i is the density in the tow i, and d_i is the midpoint of the tow depth.

2.5. Larval taxonomy

Larvae were identified using meristic characters, specifically the number of myomeres (60–65). Developmental series were illustrated using a camera lucida attached to a dissecting microscope. The best representative specimen at each stage of development (preflexion, flexion, and postflexion) was illustrated (see Kendall et al., 1984 for definition of stages). Only melanistic pigment is described because buffered formaldehyde fails to preserve other color pigments, and because pigmentation among specimens was variable, some pigment described may not be visible on the illustrations. Descriptions and illustrations of anatomical and morphometric features and other terms used herein to describe placement of pigment can be found in Matarese et al. (1989) and Moser (1996) with one exception: the area of the body between the anus and posterior edge of the hypural plates is defined as "postanal body" instead of the "tail".

Morphometric measurements were taken on the left side of the fish when possible using a calibrated digital image analysis system. The system consists of a video camera attached to a dissecting stereomicroscope or camera lens, a computer with a digital imaging board, software, and a video monitor (Blood and Matarese, 2010). Measurements made on larvae and early juveniles included: standard length (SL) as measured from the snout tip to notochord tip prior to development of caudal fin and then to posterior margin of hypural element, body depth (BD) measured as the vertical distance from dorsal to ventral body margin at the pectoral-fin origin, snout to anus length (SNA) measured as the distance along body midline from snout tip to a vertical line through center of anal opening, head length (HL) measured from the snout tip to posterior edge of opercle, snout length (SNL) measured from the snout tip to anterior margin of orbit, and eye diameter (ED) which was measured as the greatest distance of orbit.

Table 1
Cruise dates, gears, and sampling times for Greenland halibut early life stages in the eastern Bering Sea.

Year	Fish sampling	Cruise duration
2006	Bongo net, MOCNESS	8–19 May
	Beam trawl	8–23 September
2007	Bongo net, MOCNESS	7–18 May
2008	Bongo net, MOCNESS	16–27 February
	Bongo net, MOCNESS	12–21 May
2009	Bongo net, MOCNESS	21 February–2 March
	Bongo net, MOCNESS	7 May–20 May
2010	Beam trawl	2–15 September

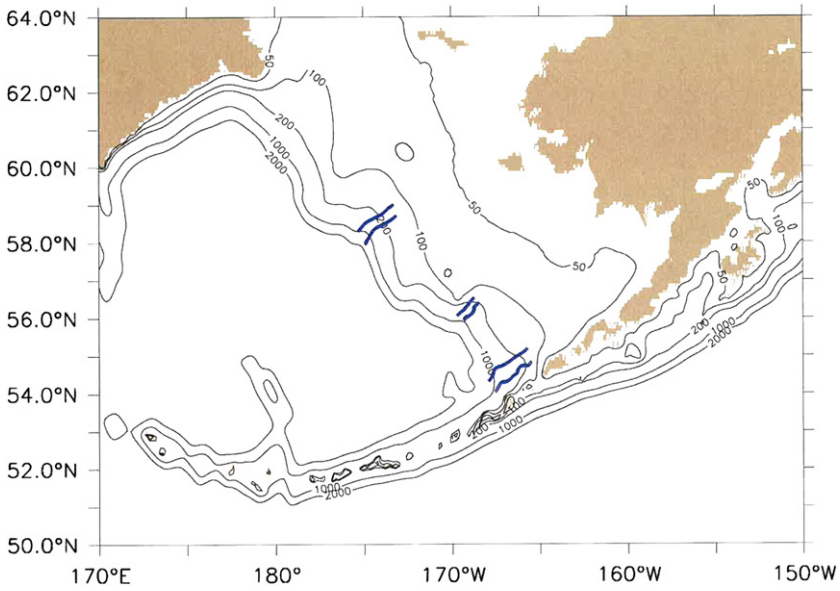

Fig. 2. Initial horizontal locations of modeled floats along Bering Slope canyons (blue lines). Floats on these locations (300) were deployed at 11 depths (0–100 m, 10 m increment), so the total number of floats simulated for each year was 3300. Isobaths of 50 m, 100 m, 200 m, 1000 m, and 2000 m in ROMS are shown by thin black lines.

Caudal-fin rays begin to develop during the yolk-sac stage when the notochord is straight and the fin rays are oriented at a near 90° angle to the notochord. Preflexion stage is protracted and flexion stage as defined for this study occurs when the following developmental hallmarks are present: caudal-fin rays visible, hypural plates visible, and the tip of the notochord is no longer in line with the rest of the body.

2.6. Modeling larval dispersal

We evaluated the potential historical (1995–2004) dispersal of Greenland halibut larvae from spawning areas in submarine canyons to nursery areas over the continental shelf using the Regional Ocean Modeling System (ROMS) circulation model (Haidvogel et al., 2000; Shchepetkin and McWilliams, 2005). ROMS is a free-surface, terrain-following primitive equation model driven by atmospheric forcing that has been used extensively to examine the effects of climate and hydrography in the North Pacific and other oceans (Curchitser et al., 2005; Di Lorenzo et al., 2008; Fiechter et al., 2009; Hermann et al., 2009). The particular grid of ROMS used in this study was NEP4, which covers the Northeast Pacific (hence the name NEP) including the Bering Sea. The horizontal resolution of ROMS NEP4 is roughly 10 km and vertically it has 42 layers, with increased resolution (i.e., smaller layer depth) near the sea surface. The implementation of ROMS NEP4 and its hindcast simulations of the Pacific Ocean for years 1996–2003 and model validations are discussed in Curchitser et al. (2005). We used ROMS to model dispersal from the beginning of the larval stage rather than from the egg stage because knowledge of egg distributions in the Pacific is limited, but information on vertical and horizontal distributions of larvae is readily available in the published literature. This approach provided more confidence in setting model initial conditions, though we acknowledge that dispersal from the egg stage to the larval stage might be significant.

We released Lagrangian floats (simulated larvae) on April 1st into the ocean in three underwater canyons, Zhemchug, Pribilof, and Bering Canyons (Fig. 2) during ROMS integrations, and the trajectories of these floats were simulated using ROMS internal particle-tracking algorithm. Although we did not attempt to collect observational data north of Pribilof Canyon during field surveys, we assumed that since Greenland halibut have a circumpolar distribution they were also likely to utilize Zhemchug Canyon as a spawning locale. Greenland halibut larvae are often collected in the top 100 m of the water column (data herein, Sohn et al., 2010) in spring, so for each of the canyons 100 floats were deployed at 11 depths (0–100 m, with 10 m increment) to examine depth-discrete variations in trajectories. In other words, altogether 3300 floats (100 floats × 11 depths × 3 locations) were released in each year. Floats were initialized from multiple locations spanning the canyons (Fig. 2) and once released into the ocean, the floats were kept at their initialization depth and their trajectories followed simulated ocean currents at that depth. Because our observations and the published literature indicate that Greenland halibut larvae tend to remain in the upper 100 m of the water column, we set the floats to drift as passive particles at a constant depth rather than follow a 3-dimensional ocean circulation which could circulate larvae to depths below known depths of occurrence. Model simulations were conducted April 1st–September 5th from 1995 to 2004, which allowed an examination of potential interannual variability. The atmospheric forcing is from the Common Ocean-ice Reference Experiments, version 2 (CORE2, available at http://data1.gfdl.noaa.gov/nomads/forms/mom4/COREv2.html). Daily locations of every simulated float were recorded during the model run.

On each day of the model simulation and for each canyon, the geographic mean center of the larval distribution for that day for each of the release depth bins was calculated using Esri's ArcGIS. The mean center of the daily distribution of floats from each release depth was taken to be representative of the mean distribution of the field of larvae. The mean center points for each depth bin for each day were connected by lines to display the path of the mean larval drift field over the temporal extent of the model run. The paths were then visualized in Esri's ArcScene to allow investigation of both the horizontal and vertical paths of the larval "clouds".

We also examined the degree of dispersion of larvae from one canyon, Bering Canyon. We illustrate dispersion by calculating the total number of particles that penetrated each of four domains (slope, outer shelf, middle shelf, inner shelf) after 1 month, 3 months,

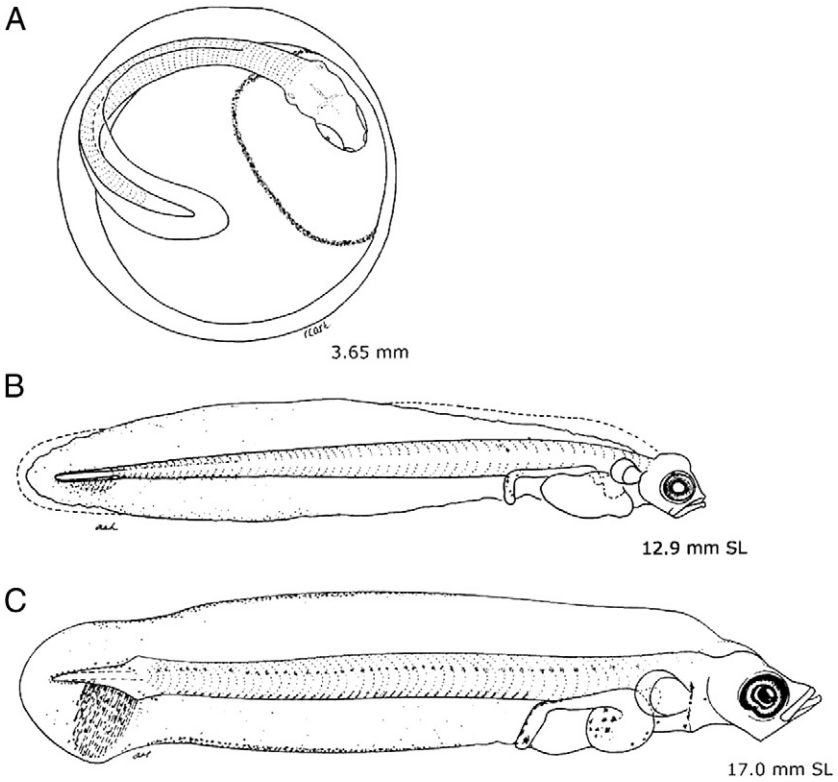

Fig. 3. Egg and larvae of Greenland halibut: (A) Late-stage egg, 3.65 mm, UW (University of Washington Fish Collection, Seattle, WA, USA) 105753; (B) yolk-sac stage, 12.9 mm SL, UW 106981; and (C) preflexion stage, 17.0 mm SL, UW 105357. A: illustrated by R. Cartwright, B–C: illustrated by A. Overdick.

and 5 months of simulation. This approach provided depth-discrete directional information that can be used to evaluate the spread of particles from the initial seed area over the slope.

3. Results

3.1. Egg and larval taxonomy description

Greenland halibut eggs are pelagic with a smooth clear chorion, homogeneous yolk, and no oil globules. Egg diameter as determined from this study is 3.50–4.30 mm. The chorion of preserved eggs may have a reddish-brown tint. The perivitelline space is narrow in early-stage eggs and may widen during later stages of development. Embryos are unpigmented throughout development. During the late stage (embryo ≥ 75% around the top of the yolk), the dorsal finfold extends anteriorly to about 5–10 myomeres behind the head and the position of the anus is about 40–50% of body length. A circle comprised of shallow depressions of irregular sizes and shapes is present on the surface of the yolk (Fig. 3). The circle (2.6–2.8 mm diameter) extends from behind the head to beyond the end of the snout, with the snout positioned at the center of the circle.

Larvae hatch at larger lengths (>6 mm) and yolk is absorbed by 17.0 mm. Preflexion larvae range in size from 6.8 to 19.2 mm. Notochord flexion in Greenland halibut can begin at the end of the yolk-sac stage. Flexion larvae are 16.9–21.9 mm; postflexion larvae are 22.9–50.9 mm (Fig. 4). Transformation occurs at lengths as large as 45–65 mm and left eye migration may not be complete until >70 mm. The juvenile stage begins before 53 mm and the transformation post-settlement juvenile stage is attained after 72 mm. Relative mean head length (10.0–26.9% SL), snout length (20.9–30.4% HL), and body depth (5.1–21.0% SL) increase with development, sharply after flexion (Table 2). Relative mean eye diameter (49.9–17.2% HL) decreases throughout development. Relative mean snout-to-anus length decreases from 36.8% SL during preflexion to 34.2% SL during flexion, then increases to 38.0% SL during postflexion. Total number of myomeres is 60–65.

Greenland halibut larvae are distinct from all other pleuronectid larvae in the Northeast Pacific by their high myomere counts (≥60), overall light pigmentation pattern and lack of a specific band pattern. Newly hatched yolk-sac larvae are unpigmented except for the eye. With development, light pigment is added laterally on the hindgut. The dorsal and anal finfolds are speckled with melanophores from midbody around the tail.

In preflexion and flexion larvae (<20 mm), preanal pigment is present initially just posterior to opercle and along the cleithral region, increasing with development to the hindbrain, lower jaw, opercular region and isthmus (Fig. 3). Pigment is present anteriorly along the gut, laterally where the gut coils, and dorsally on hindgut and anal tip. By the flexion stage melanophores appear along the posterior edge of the gut and pigment increases laterally with development. Postanal pigment is present as melanophores along the distal edges of dorsal (posterior 3/4 length) and anal finfolds. Initially a double row of postanal ventral melanophores (PVM) occurs along hypaxial muscles on the posterior 25% of the body and a series of internal melanophores is present above the notochord in the same area. By the flexion stage, the double row of PVM is present from the gut along the ventral midline to the caudal area and the internal melanophores extend from midgut to the last 1–2 myomeres.

In postflexion and transforming larvae (about 22–50 mm), overall pigment remains light until the juvenile pigmentation pattern begins to develop (Fig. 4). Initially, dark pigment bars appear in the dorsal and anal fin rays and pterygiophores. With development, the melanophores associated with the pigment bars migrate to along the epaxial and hypaxial musculature. Melanophores continue to increase on the head

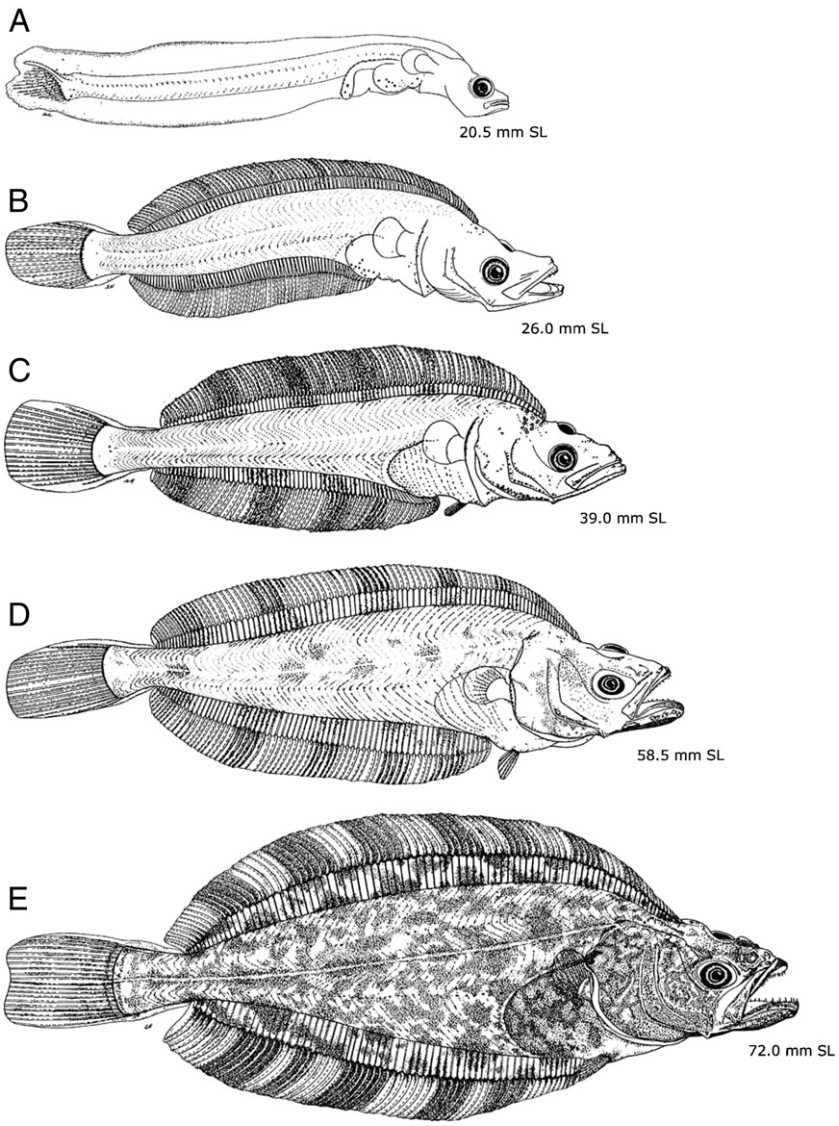

Fig. 4. Larvae of Greenland halibut: (A) flexion stage, 20.5 mm SL, UW (University of Washington Fish Collection, Seattle, WA, USA) 105355; (B) postflexion stage, 26.0 mm SL, UW 105346; (C) late postflexion stage, 39.0 mm SL, UW 105351; (D) early transformation stage, 58.5 mm SL, UW 105899; and (E) late transformation stage, 72.0 mm SL, UW 105908. Illustrations by A. Overdick.

and body, eventually becoming typical juvenile coloration with pigment bars in the dorsal and anal fins and mottled pigment patches on the body.

3.2. Egg and larval distributions

Greenland halibut eggs are present in the water column in late winter in the southeastern Bering Sea (Fig. 5). Eggs were commonly collected over the basin and in submarine canyons (Bering, Pribilof), and limited depth-discrete tow collections suggest eggs are predominantly found 200 m–400 m depth (Fig. 6A), though it should be noted that maximum tow depth for the MOCNESS was only 500 m. Selected bongo tows occurred deeper, to a depth of 600 m, and staging efforts from these tows indicated that earliest stages were collected from deeper tows (Fig. 6B). Stage-specific calculations of CWMD of eggs collected from bongo tows determined depths of 246 m, 207 m, and 234 m for Early, Middle, and Late Stage eggs, respectively.

No eggs were collected over the continental shelf, but by spring Greenland halibut larvae were more dispersed and occurred over the basin, shelf break, canyons, and the outer continental shelf. Larvae were present in the water column February–May and settled juveniles were collected in September on the middle and outer continental shelves (Fig. 5). Limited data derived from MOCNESS sampling indicated that preflexion stages of Greenland halibut larvae were collected at depths >300 m in February, but by May postflexion stages were found <50 m depth, indicating an ascent through the water column post-hatching (Fig. 6C).

3.3. Modeling larval dispersal

Before using the ROMS simulated floats to study larval dispersal, we compared ROMS simulated velocity field with observations derived from the field. We used data derived from satellite-tracked drifter deployments (1995–2004) conducted by the Fisheries Oceanography Coordinated Investigations (FOCI) Program, NOAA Alaska Fisheries Science Center and Pacific Marine Environmental Laboratory, for this comparison http://www.ecofoci.noaa.gov/drifters/efoci_drifterData.shtml. Drifters were drogued at 40 m depth and their hourly positions were tracked by satellite; these locations were used to calculate local velocity. The observed and modeled velocities (also at 40 m depth) between April 15th and September 15th of each year were binned into the same 0.5°×0.5° longitude–latitude grid in the Bering Sea. Only bins

Table 2
Body proportions of *Reinhardtius hippoglossoides* larvae. Except for standard length, values given for each body proportion are expressed as percentage standard length (SL) or head length (HL): mean ± standard deviation, and range (in parentheses).

	Preflexion		Flexion		Postflexion	
Sample size	44		15		30	
Standard length (mm)	12.0 ± 3.3	(6.8–19.2)	20.0 ± 1.4	(16.9–21.9)	34.0 ± 6.6	(22.9–50.9)
Head length/SL	10.0 ± 3.0	(5.9–15.7)[a]	16.8 ± 1.8	(12.2–19.5)	26.9 ± 2.3	(20.2–29.7)[b]
Snout length/HL	20.9 ± 5.1	(11.3–34.7)[a]	23.3 ± 2.7	(18.7–27.6)[c]	30.4 ± 3.2	(23.7–39.1)[b]
Eye diameter/HL	49.9 ± 15.2	(28.1–79.9)[d]	26.2 ± 3.6	(21.9–37.2)	17.2 ± 2.0	(13.6–22.0)
Snout to anus length/SL	36.8 ± 4.4	(30.2–49.6)[4]	34.2 ± 1.2	(32.4–36.1)	38.0 ± 2.3	(33.0–42.0)
Body depth/SL	5.1 ± 0.7	(3.5–6.6)	5.5 ± 0.8	(4.1–6.8)	21.0 ± 3.5	(14.4–28.3)[e]

[a] $n = 42$.
[b] $n = 29$.
[c] $n = 14$.
[d] $n = 43$.
[e] $n = 28$.

with more than 150 observational data were used for model–data comparison. While model simulated ocean velocity (Fig. 7A) captured the observed major current systems including the Alaska Stream located south of the Aleutian Islands, the northeastward flowing Aleutian North Slope Current, and the Bering Slope Current moving northwestward along the shelf break, the probability distribution function (PDF) of the ratio of the simulated over observed current amplitude is skewed toward values <1.0 (Fig. 7B). This indicates that on average, the simulated currents are weaker than observations, even though the majority of model-to-observation ratios still fall within 0.5–1.5. This type of model bias is expected for a model with relatively coarse horizontal and vertical resolutions like the one used in this study. Generally however, the modeled current directions are in good agreement with observations (Fig. 7C), with the model simulation showing somewhat stronger topographic steering effects than observations. These model biases should be kept in mind when interpreting modeling results.

Data derived from numerical modeling suggest that horizontal movement of larvae varies by depth. Generally within any given year, mean dispersal pathways of floats initialized at deeper depths (50–100 m) were comparable to one another, while trajectories of floats initialized <30 m depth tended to be significantly more variable (Figs. 8, 9, 10). Occasionally floats initialized within the wind mixed layer (0–30 m) moved far over the middle and even inner shelves (Bering Canyon, 1998, 1999; Pribilof Canyon, 1997, 1998, 2003), and Zhemchug Canyon (1998, 2003). In several instances this significant wind-induced penetration was simultaneously coupled with retention of floats seeded >30 m over the slope and basin, providing a significant discrepancy in the end points of floats seeded above 30 m depth and those seeded deeper (Bering Canyon, 1998–2001; Pribilof Canyon 1997, 1998, 2003).

Penetration of floats to the shelf was observed in all canyons, though variability in degree was observed. Greatest variability was observed in the Bering Canyon region. From this initialization area,

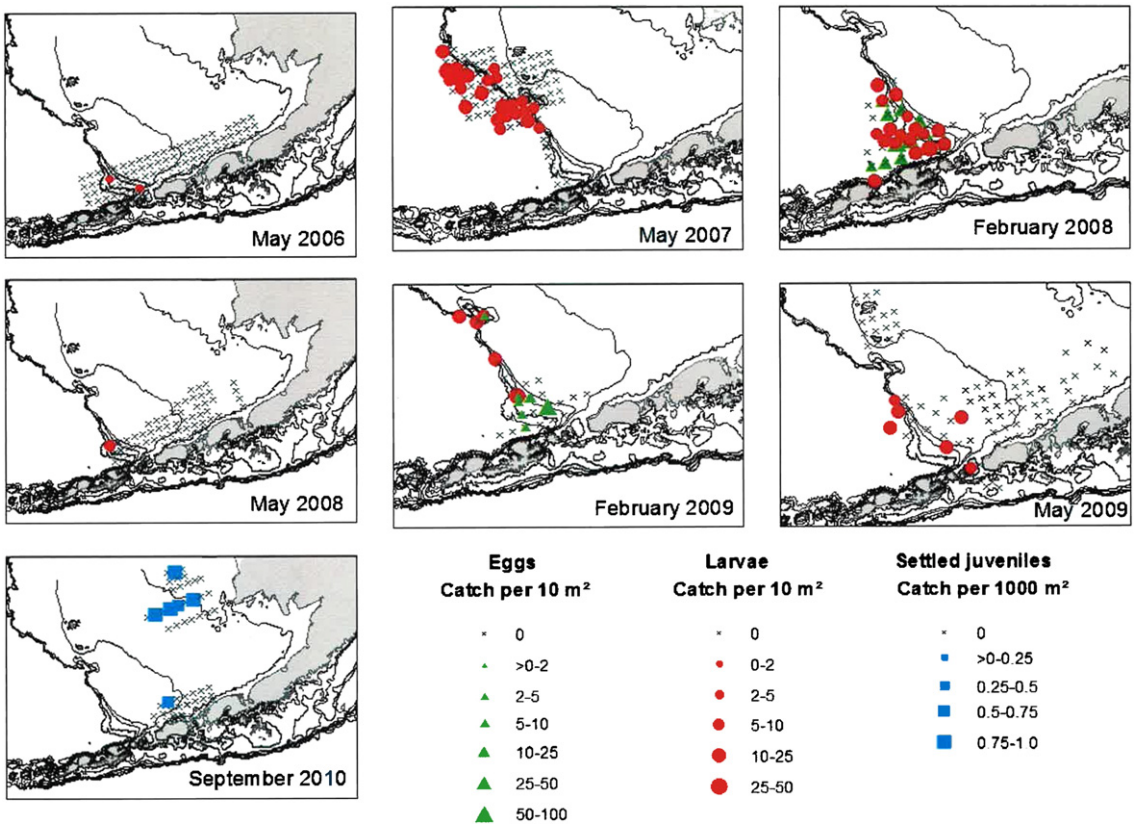

Fig. 5. Seasonal geographic distribution of Greenland halibut eggs (triangles), larvae (circles), and juveniles (squares). Eggs and larvae were collected in plankton tows, juveniles were collected from beam trawls (2006–2010).

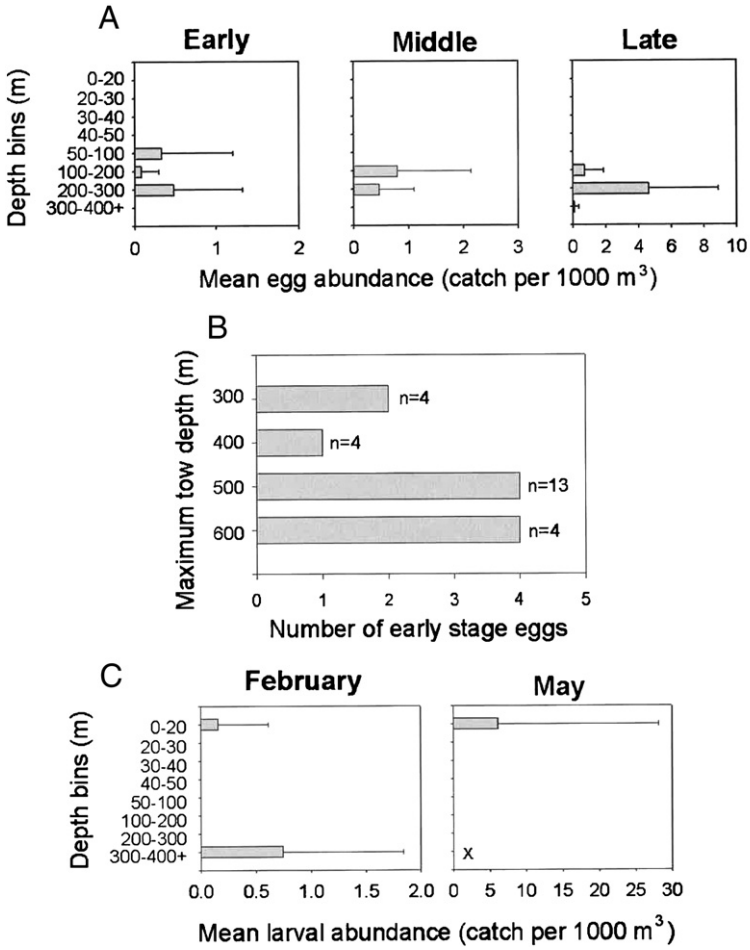

Fig. 6. A. Mean abundance (±standard deviation) of Greenland halibut eggs collected in MOCNESS tows by developmental stage and depth. Early Stage (left), Middle Stage (middle), and Late Stage (right). B. Number of Early Stage Greenland halibut eggs collected from bongo tows. N indicates number of tows conducted. C. Mean abundance (±standard deviation) of Greenland halibut larvae collected in MOCNESS tows by month and depth. "X" indicates depth not sampled. No larvae were collected in September (not shown).

selected years showed little or no advection over the shelf (1995, 1996, 1999, 2001, 2003), while others demonstrated transport as far as the middle and inner shelves (1998, 1999, 2004). It was also observed that floats initialized in Pribilof Canyon appeared to have the strongest penetration onto the shelf, particularly in years 1997, 1999, 2000, 2001, and 2002 (Fig. 9). Eastward penetration of floats initialized in Zhemchug Canyon was least, with successful floats penetrating only as far as the outer shelf (Fig. 10). However, unlike Bering and Pribilof Canyon, floats from the Zhemchug region exhibited regular, albeit small, on-shelf transport from the basin to the shelf, indicating that on-shelf flow from this area is interannually consistent. It should be noted however, that though float trajectories from Zhemchug Canyon crossed to the shelf at some point during their journey, paths often re-crossed back to the slope such that endpoints on the last day of the simulation were over the basin/slope (1995, 1996, 1999, 2000, 2002, 2003, 2004), suggesting that opportunity for Greenland halibut to settle over the shelf from Zhemchug Canyon is temporally limited. In Pribilof and Bering Canyons, if floats crossed to the shelf they tended to be retained there, potentially providing greater temporal opportunity for settlement.

Variability of individual floats from the mean center of distribution was high across all years and depths. Surface floats tended to have greater variability than floats initialized below the pycnocline (20 m). An example is provided for Bering Canyon. After 1 month of simulation an average of only 53% of floats occurred over the slope (initialization area), with 31% being transported to the outer shelf, 15% to the middle shelf and 2% penetrating as far as in the inner shelf (Table 3). At 100 m depth, nearly 65% of the floats initialized at that depth were retained over the slope, with fewer than 1% of particles penetrating the inner shelf. After 5 months of simulation, a full 35% of particles initialized in the surface waters had penetrated in the middle and inner shelves, though the mean trajectory pathway for all years indicates average penetration only as far as the outer continental shelf. These results indicate that variability around the mean pathway can be considerable.

4. Discussion

Our approach, which combines field and laboratory methodologies with circulation modeling, has demonstrated that: 1) Greenland halibut spawning in the Bering Sea occurs in proximity to undersea canyons in winter, 2) eggs, 3.5–4.3 mm diameter, primarily occur 300–400 m deep; larvae are distinctive and reach some developmental milestones at smaller sizes than their Atlantic counterparts, and 3) degree of transport connectivity of larvae between the slope and the shelf is spatially and temporally varied. Observations are based on limited field sampling (2006–2010), though they are consistent with conclusions from an earlier study (Sohn et al., 2010). Prior to this work, there were few historical data on Greenland halibut egg distributions in the Bering Sea and no recent data, and little information on the development of early life stages in this region. Our study provides new information on the development, seasonality, vertical distribution, and dispersal Greenland halibut of early life stages in the North Pacific.

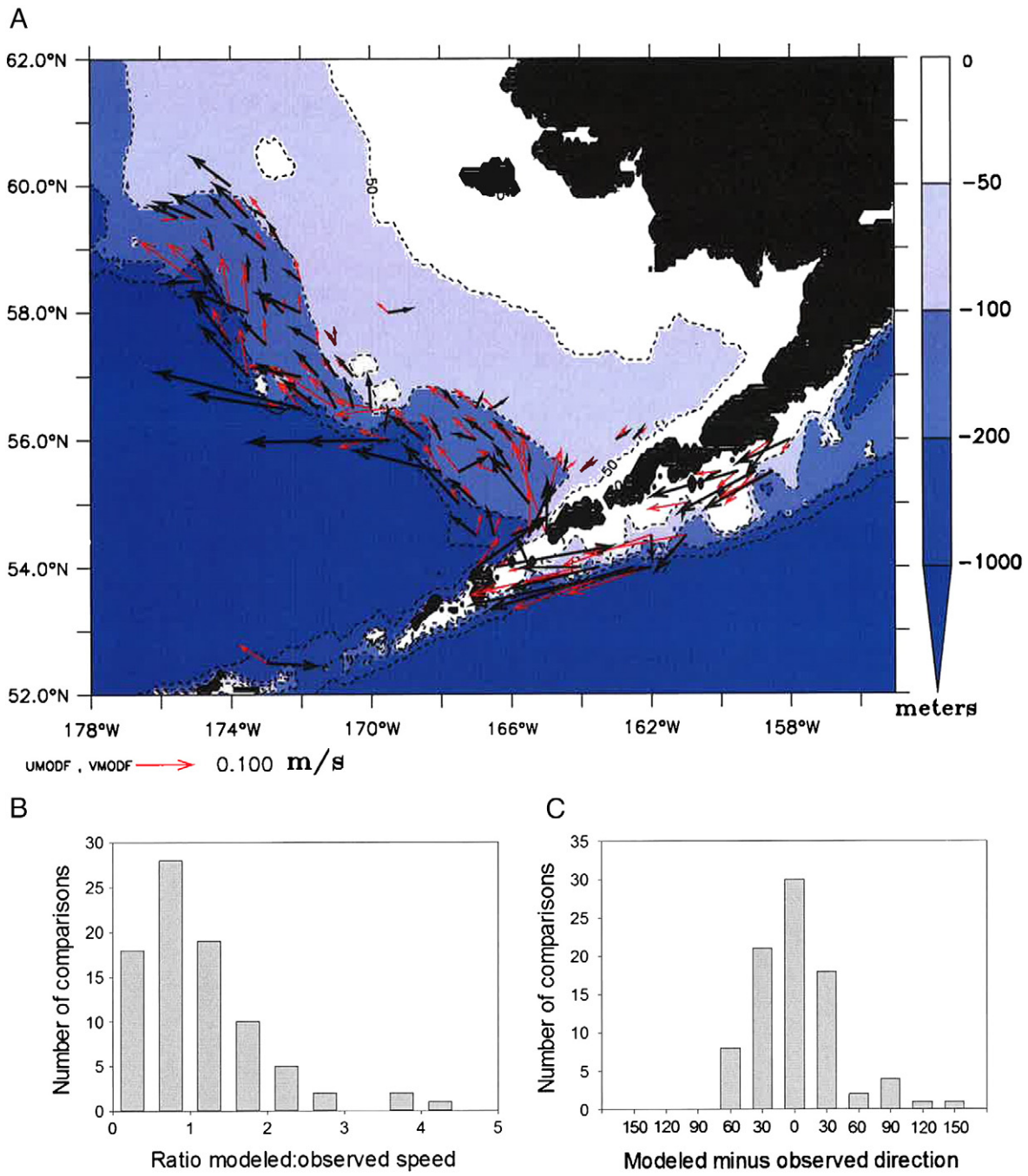

Fig. 7. A. Comparison of modeled (red) and drifter-derived (black) ocean velocity vectors at 40 m depth. Blue shading indicates ocean bathymetry. Observed and modeled data from April 15 to September 15 (1995–2004) were binned into 0.5°×0.5° bins. Only results with more than 150 observational and modeled data points in each bin and <1000 m are shown. B. Probability distribution function (PDF) of the ratio of modeled over observed current speed at 40 m depth. Total number of comparisons = 85. C. PDF of modeled minus observed current directions; total number of comparisons = 85.

4.1. Development

Observations of field-caught Greenland halibut eggs in previous studies have been based on few specimens. Eggs collected from the Atlantic Ocean and Barents Sea were 3.7–4.7 mm in diameter and chorions of some eggs were reddish-brown, whereas other eggs had no color (Fahay, 2007; Stene et al., 1999). Eggs collected from the Bering Sea during previous studies were 3.71–4.10 mm and were reddish-brown in color (Bulatov, 1983), though eggs collected during this study were 3.5–4.3 mm with both reddish-brown chorions and chorions with no color.

Overall, morphological and pigment development of Bering Sea larvae occurs at smaller sizes than larvae from the Atlantic and other locations. This may be due, in part, to the smaller sizes of eggs in the Bering Sea. Our 12.9 mm larva has pigment similar to the 16 mm larva in Jensen (1935), and, in addition, has pigment in the dorsal and anal finfolds extending further forward to midbody. Our 17 mm larva shows fine pigment at the edge of the dorsal and anal finfolds that is not apparent until 25 mm in Jensen (1935). Our 26 mm larva is more developed than the same length larva in Jensen (1935), with fully formed dorsal and anal-fin rays, notochord not visible, posterior edge of hypural plates vertical, and left eye

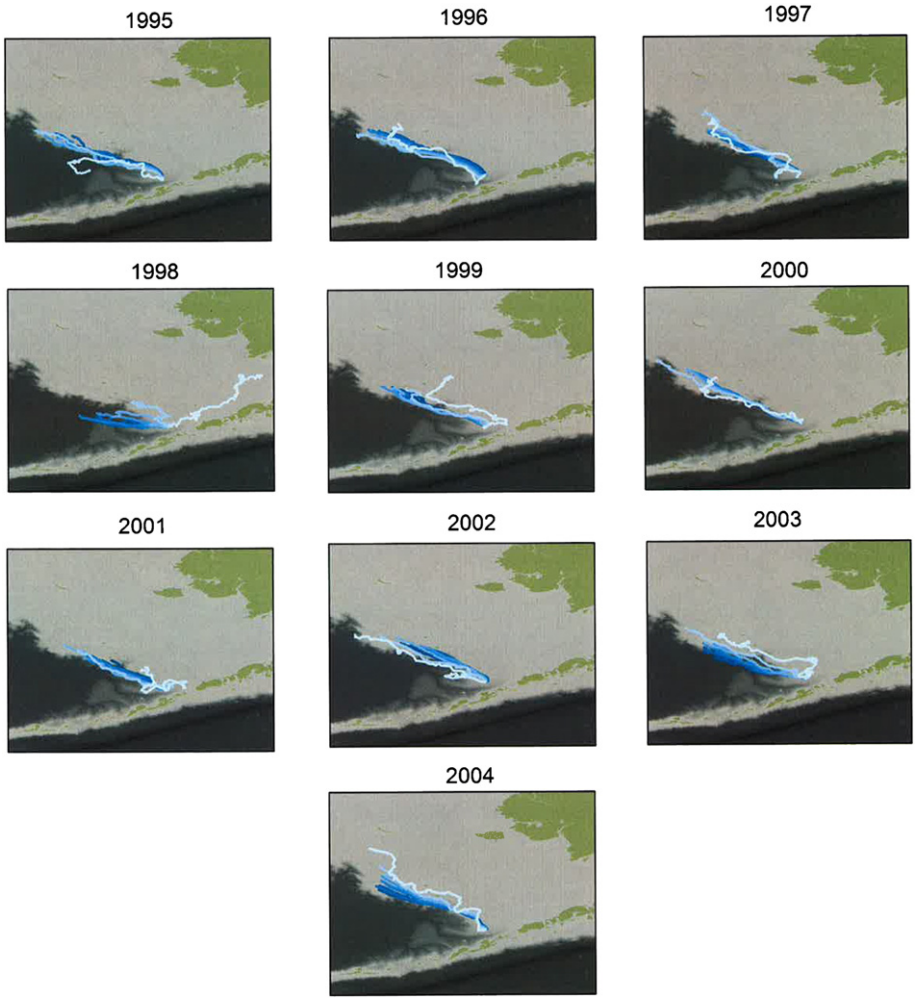

Fig. 8. Mean pathways of the modeled particles (larvae) released in Bering Canyon 1995–2004. The lightest blue paths show the particles released at the shallowest depth and the path color darkens for successively deeper release points (0–100 m).

visible from the eyed side. Fully formed dorsal and anal fins are not shown until 57 mm in Jensen (1935), but are illustrated in a 36.5 mm larva in Schmidt (1904). Pelvic fins are developed by 39 mm in our larvae; small pelvic fins are shown in a 50 mm larva from the western Pacific (Tsukamoto et al., 1995), but do not appear on specimens from the Atlantic until 57 mm (Jensen, 1935). Reasons for differences in size at ontogenetic stage between systems are unknown, but could be related to differences in temperatures, predation pressure, variations in population or prey density or genetic differences.

4.2. Seasonality and horizontal distribution

Our field survey data suggest that Greenland halibut spawning in the southeastern Bering Sea occurs over the continental slope in winter, with most spawning activity completed by late February. This conclusion is based on two findings. First, that Greenland halibut eggs were collected exclusively in February and were primarily in later stages of development, suggesting that spawning occurred a few weeks prior. However, it should be noted that maximum tow depths were generally 500–600 m, and eggs in earlier stages of development could have occurred at depths deeper than those sampled (Stene et al., 1999). Second, limited trawling activities to collect spawning condition male and female Greenland halibut (February cruises, trawl depths 400–800 m) determined that all females were in post-spawning condition. Females were flaccid and ovaries contained only a few, remnant, hydrated eggs. Male Greenland halibut were collected in ripe and running condition during the first week of each research cruise, but individuals collected during the second week of field research were spent. These two lines of evidence suggest that spawning occurs some weeks prior to the end of February, and corroborate spawning hypotheses postulated in a retrospective study of Greenland halibut early life ecology in the Bering Sea (Sohn et al., 2010).

Unlike eggs that were only collected over the slope in winter, Greenland halibut larvae were collected over both the slope and shelf in spring, indicating seasonal advection to at least the outer continental shelf. We noted that postflexion larvae occurred in the upper 20 m of the water column and model results suggest that larvae retained above 30 m depth, the approximate depth of the wind mixed layer, are potentially transported farther over the continental shelf during spring than the larvae occurring below 30 m. However, considerable inter-annual variability exists in the on-shelf transport in both the wind-driven and deeper layers (see below, *Physical environment*). Nevertheless, settled juveniles were collected far over the middle shelf in autumn suggesting additional horizontal movement through the summer.

Interestingly, limited sampling of settled juveniles in the present study demonstrates the presence of benthic juveniles over the Cape Newenham region of the middle and inner shelves, farther inshore and more southerly than previously reported (Sohn et al., 2010). It is interesting to note that 2010 was during a prolonged cold period (2007–2011; Stabeno et al., 2012), suggesting that Greenland halibut larvae and juveniles may have been able to

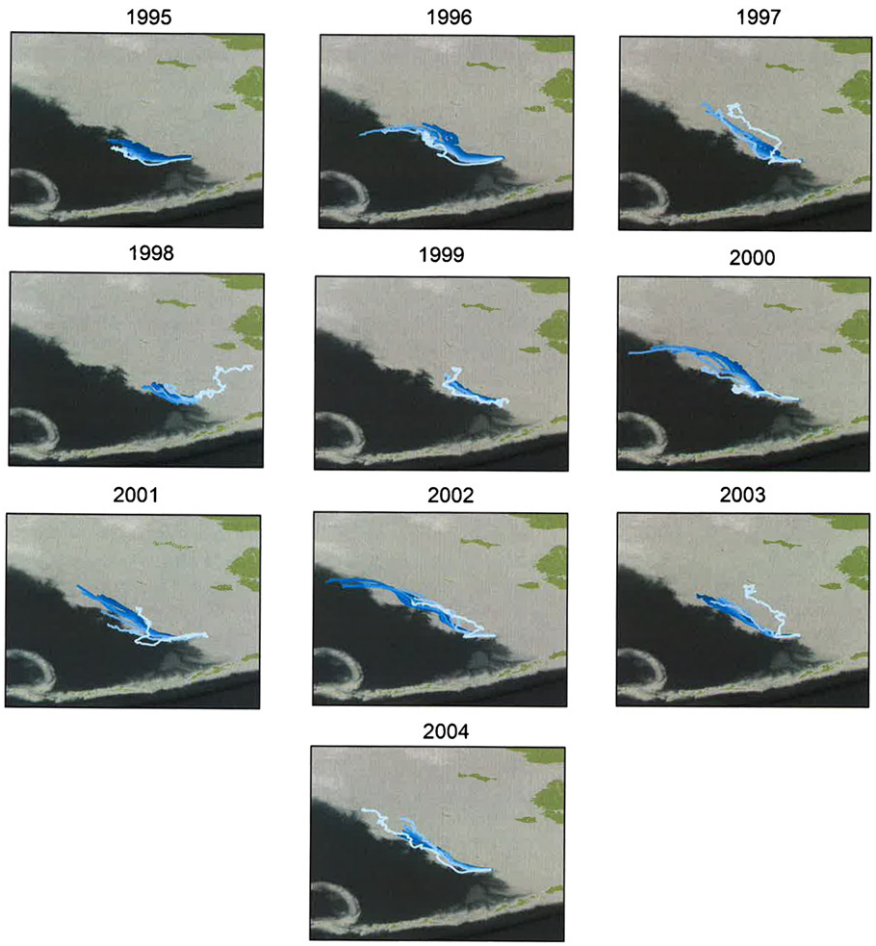

Fig. 9. Mean pathways of the modeled particles (larvae) released in Pribilof Canyon 1995–2004. The lightest blue paths show the particles released at the shallowest depth and the path color darkens for successively deeper release points (0–100 m).

penetrate southwards to areas not recently available as suitable nursery ground. Data on distributions of adults collected by the NOAA Fisheries Groundfish Assessment Program summer bottom trawl surveys (summarized in Ianelli et al., 2011) support this hypothesis and indicate highest catches and most southerly extent of Greenland halibut over the middle shelf in 2010. The Bering Sea has generally experienced a prolonged warming trend (Grebmeier et al., 2006), though the years from 2007 to 2011 present a short-term deviation from this assessment and were generally cold (Stabeno et al., 2012). Information on extent of adults (2003–2010) suggests that it was only in 2010 that summer distributions reached as far south as the Pribilof Islands (Ianelli et al., 2011); though we collected eggs as far south as Bering Canyon in winter in all field years. Summer and winter distributions of adult Greenland halibut may differ (Vestfals, personal communication) and it may be that adults spawn in southerly areas in winter when temperatures are low but move north if thermal conditions later in the year are not ideal. In any case, we noted settled distributions of age-0s suggesting that, at least in 2010, broad portions of the southern middle and inner shelves were utilized as nursery areas.

4.3. Vertical distribution

Most previous studies of egg distribution have used only depth-integrated sampling gear so reported depth of collection of eggs has included the entire water column from the maximum depth of the gear (600–3000 m) to the surface (Stene et al., 1999). One exception has been a report of eggs collected at 850–1000 m near Iceland (Magnusson, 1977). Depth-discrete sampling used in this study shows that Greenland halibut eggs are collected most frequently at 200–300 m. Eggs were found as deep as 300–400 m and as shallow as 50–100 m, however, when combined these represented only 3% of the total. No eggs were found below 400 m in MOCNESS samples, though staged eggs from bongo tows conducted to depths of 600 m did have eggs in earlier stages of development. A limitation of our depth-discrete sampling was that samples were only collected as deep as 500 m. Previous work in the north Atlantic has indicated that eggs can occur >500 m (Magnusson, 1977) so our sampling may have missed the deepest, most recently spawned eggs. Indeed, limited data from bongo tows conducted to 600 m indicated the presence of earlier stages deeper in the water column. Developmental changes in Greenland halibut egg buoyancy and vertical position have been documented in the laboratory (Stene et al., 1999), though trends from this study are not robust. Additional vertically-stratified sampling several weeks earlier in the spawning season and at deeper depths would help to confirm the general observations presented here.

4.4. Physical environment

Greenland halibut, as well as other slope-spawning species with nursery areas over the adjacent shelf, must transport their larvae horizontally across the northwestward flowing Bering Slope Current, and vertically from depth, to ensure survival of offspring. Larval Greenland halibut are at risk of protracted entrainment in the Bering Slope Current, which could transport propagules along isobaths at the slope–shelf margin rather than across them to juvenile nursery areas on the continental shelf. Spawning in and near underwater canyons may mitigate

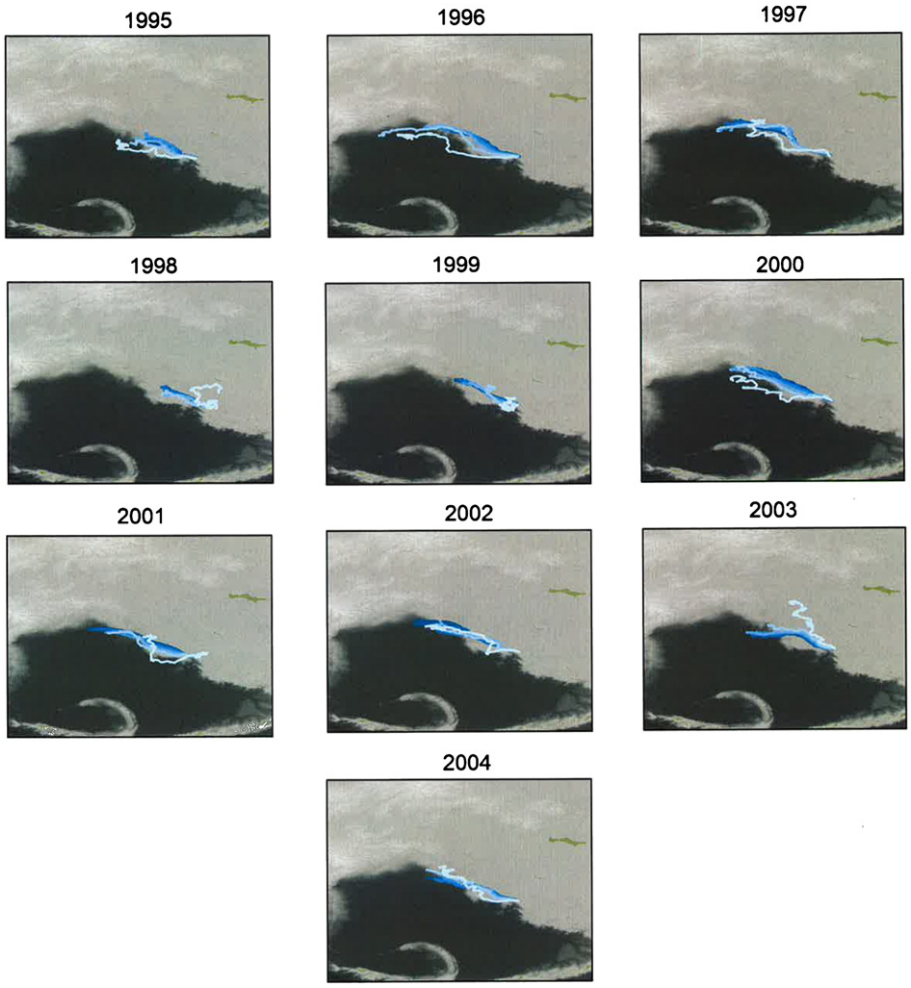

Fig. 10. Mean pathways of the modeled particles released in Zhemchug Canyon 1995–2004. The lightest blue paths show the particles released at the shallowest depth and the path color darkens for successively deeper release points (0–100 m).

a portion of that risk as canyons can act to modify regional currents, increasing the likelihood that larvae are advected to the shelf. In particular, topographically-controlled flow in the vicinity of submarine canyons contributes to enhanced mixing (Carter and Gregg, 2002), upwelling (Allen and Hickey, 2010; Kämpf, 2005), the generation of internal waves (Kunze et al., 2002), and enhanced shelf-break exchange (Hickey and Banas, 2008), all of which foster vertical and horizontal advections. These observations support the generalized hypothesis that fishes spawn in areas with persistent oceanographic features that support delivery of propagules (Iles and Sinclair, 1982). However, our model analysis demonstrates that despite spawning in areas generally conducive to larval transport, there is considerable interannual variability in the degree of slope–shelf connectivity, at least for two of the three canyons studied. The source of these interannual variations is as yet unresolved, but ongoing research (Vestfals, unpublished) shows that strong seasonal and interannual variations in the BSC are apparent, with along-shelf transport generally highest during fall and winter months, which coincides with Greenland halibut spawning activity. In warm years when sea ice retreats before early March (Stabeno et al., 2012), the BSC current appears stronger and closer to the shelf break than in cold years, when extensive sea ice persists through April.

Model output also indicates that mean float trajectories vary with depth and among years. Depth-discrete variations were expected, as wind-forcing generally governs the top 30 m or so of water movement in the Bering Sea, while baroclinic forcing and geostrophic flows regulate currents at depth (Stabeno et al., 1999). Interannual variabilities in wind strength and direction likely drive the year-to-year differences in on-shelf flow of floats above 30 m depth, however we also observed differences in mean flow below 30 m. In particular, selected years demonstrated increased penetration of floats initialized at depth >30 m to the outer shelf, though the specific years were not consistent among canyons. For example, in Bering and Pribilof Canyons the years 2002–2004 appeared to show the most penetration, while for Zhemchug Canyon 1995–1998 were the strongest. Fundamental oceanographic and biological differences exist between the northern (north of 60°N) and southern Bering Sea, including ice presence and the influence of selected regional currents (Sigler et al., 2011; Stabeno et al., 2012), which could contribute to the observed dissimilarities. Interestingly, significant on-shelf advection (2002–2004) from canyons in the southern Bering Sea (Bering, Pribilof) coincides with documented anomalously warm conditions (2002–2005) characterized by low ice extent during spring and predominantly westward currents over the shelf (Stabeno et al., 2012). We hypothesize that slope–shelf connectivity over the southern shelf may be improved during warm periods, though additional work to verify observations and elucidate mechanisms is necessary.

Mean float trajectories from Zhemchug Canyon consistently crossed to the outer continental shelf, though trajectories tended to return to the basin by the conclusion of the model simulation. While consistent connectivity to the continental shelf would generally be construed as beneficial to Greenland halibut larvae, it may be ineffective if ontogenetic development has not sufficiently progressed to a point where larvae have attained settlement readiness. Greenland halibut have a long larval pelagic period (>6 months, Bowering and Nedreaas, 2000; Sohn et al., 2010) with settlement likely occurring at large sizes, 70–100 mm SL

Table 3
Dispersion. Average number of simulated larvae occurring in each of four domains (slope, outer continental shelf, middle continental shelf, and inner continental shelf) after 1 month (A), 3 months (B), and 5 months (C) of particle tracking (1995–2004). Initial densities were 100 simulated larvae at each depth (0–100 m) in Bering Canyon (slope).

Depth	Slope	Outer shelf	Middle shelf	Inner shelf
A.				
0 m	52.8 (31.7)	30.9 (23.1)	14.6 (23.5)	1.7 (2.4)
10 m	59.9 (24.1)	35.0 (19.5)	4.7 (6.3)	0.4 (0.5)
20 m	65.3 (19.1)	33.0 (17.9)	1.5 (2.7)	0.2 (0.4)
30 m	67.3 (16.7)	31.4 (15.6)	0.9 (1.6)	0.4 (0.7)
40 m	64 (14.7)	32.3 (13.2)	1.9 (0.8)	1.8 (1.7)
50 m	66.1 (14.3)	31.3 (12.4)	2.0 (1.9)	0.6 (0.9)
60 m	62.4 (12.8)	34.3 (11.7)	2.4 (2.4)	0.9 (1.7)
70 m	60.8 (12.3)	35.8 (11.4)	2.5 (1.4)	0.9 (1.3)
80 m	61.4 (9.8)	37.1 (9.2)	1.2 (1.4)	0.3 (0.7)
90 m	60.5 (7.1)	36.5 (5.9)	2.2 (0.8)	0.8 (0.6)
100 m	63.5 (4.4)	34.0 (4.1)	2.2 (1.3)	0.3 (0.4)
B.				
0 m	47.1 (28.8)	22.1 (19.2)	22.3 (26.1)	8.5 (11.9)
10 m	56.5 (24.5)	33.7 (18.2)	7.8 (11.4)	2.0 (2.8)
20 m	58.5 (15.5)	36.9 (14.2)	3.6 (4.8)	1.0 (0.7)
30 m	56.7 (11.1)	39.7 (11.3)	2.7 (3.0)	0.9 (0.8)
40 m	59.2 (12.8)	36.7 (12.3)	2.4 (4.0)	1.7 (1.6)
50 m	59.5 (12.7)	35.7 (12.6)	3.5 (3.4)	1.3 (0.9)
60 m	58.3 (9.3)	36.0 (9.3)	4.0 (3.0)	1.7 (1.4)
70 m	57.7 (9.7)	38.0 (9.4)	3.1 (2.3)	1.2 (1.4)
80 m	62.1 (12.7)	35.0 (13.1)	2.1 (2.4)	0.8 (0.8)
90 m	61.4 (8.7)	34.5 (9.1)	2.8 (2.2)	1.3 (0.9)
100 m	64.1 (8.4)	31.7 (10.1)	3.4 (3.0)	0.8 (1.1)
C.				
0 m	43.1 (25.2)	22.1 (18.3)	22.6 (22.5)	12.2 (20.1)
10 m	55.1 (21.6)	35.0 (17.0)	8.2 (11.5)	1.7 (2.8)
20 m	59.1 (14.0)	34.9 (16.3)	4.4 (4.7)	1.6 (2.1)
30 m	57.4 (9.8)	38.7 (11.7)	2.7 (2.8)	1.2 (1.4)
40 m	56.7 (10.3)	37.1 (12.2)	3.7 (3.8)	2.5 (1.4)
50 m	56.5 (11.3)	38.1 (12.6)	4.4 (3.8)	1.0 (0.9)
60 m	55.7 (6.8)	38.2 (8.0)	4.2 (2.8)	1.9 (1.6)
70 m	55.7 (7.7)	39.3 (9.4)	3.9 (2.2)	1.1 (1.3)
80 m	59.0 (9.1)	37.5 (10.0)	2.7 (2.3)	0.8 (0.6)
90 m	58.8 (7.3)	37.6 (7.9)	2.7 (2.2)	0.9 (0.8)
100 m	60.6 (7.9)	35.1 (9.0)	3.4 (2.9)	0.9 (1.1)

(Sohn, unpublished data). Model output demonstrates that advection to the outer shelf can occur as early as April, suggesting that at least in some instances, Greenland halibut larvae may not be competent to settle. If these underdeveloped larvae are retained in currents that eventually return to the continental slope, larvae are at risk of becoming competent far out over the Aleutian Basin and away from appropriate nursery habitat. Trajectories emanating from Bering and/or Pribilof Canyons however, showed more interannual variability in basin–shelf connectivity, but, once over the shelf, mean float trajectories tended to remain there providing greater opportunity for larvae to continue development over large swaths of suitable nursery habitat. Finally, given the systematic biases in ROMS simulated ocean velocities (on average, weaker currents and stronger topographic steering than observations), our results likely only give a low-end estimation of onto-shelf transport, while the real world presents stronger slope–shelf connectivity.

A limitation of our modeling efforts was the lack of behavioral information to implement an individual based model (IBM) within the ROMS 3-dimensional hydrodynamic model. Such a simulation would have allowed greater flexibility in incorporating potential vertical movements of larvae in response to prey, light, predators or other factors. However, given the paucity of information on Greenland halibut behavioral ecology in the Bering Sea, such an effort would have required adopting data from other systems as proxy data, which was deemed inappropriate for the present effort. However, as new information on egg and larval vertical distribution becomes available, an IBM may offer new insights into connectivity between spawning and nursery grounds.

Overall, our results provide new information on the distribution and development of early life stages of Greenland halibut in the eastern Bering Sea, and provide evidence that interannual variability in currents and thermal regime play a role in their distribution and habitat use. In particular, we suggest that physical mechanisms of delivery of eggs and larvae can be modulated by large-scale atmospheric and oceanographic forcing, which varies the degree of slope–shelf connectivity for Greenland halibut and potentially other species that spawn over the basin and continental slope.

Acknowledgments

This work was supported by the North Pacific Research Board, Grants #619 and #905, by NOAA's North Pacific and Climate Regimes and Ecosystem Productivity (NPCREP) program, and the Alaska Fisheries Science Center's Resource Assessment Conservation and Engineering Division. Gratitude is expressed to Enrique Curchitser (Rutgers University) and Kate Hedstrom (University of Alaska) for the development and use of the ROMS (NEP4 version). Thank you to Zachary Winters-Staszak for the valuable assistance in plotting the mean trajectory pathways. Thanks to the officers and crew of the NOAA Ships *Miller Freeman* and *Oscar Dyson* for their efforts in the field. Three anonymous reviewers provided comments on earlier versions of this manuscript. This is NPRB contribution number XX and contribution N738-RAOAP to NOAA's Ecosystems and Fisheries-Oceanography Coordinated Investigations program.

References

Ádlandsvik, B., 2000. Modeling transport of eggs and larvae of Greenland halibut in east-Greenland waters. In: Woll, A.K., Boje, J., Hjorleifsson, E., Gundersen, A.C. (Eds.), Greenland Halibut in East Greenland Waters. TemaNord 2000, 585. Nordic Council of Ministers, Copenhagen, pp. 49–78.

Ådlandsvik, B., Gundersen, A.C., Nedreaas, K.H., Stene, A., Albert, O.T., 2004. Modelling the advection and diffusion of eggs and larvae of Greenland halibut (*Reinhardtius hippoglossoides*) in the north-east Arctic. Fisheries Oceanography 13 (6), 403–415.

Allen, S.E., Hickey, B.M., 2010. Dynamics of advection-driven upwelling over a shelf break submarine canyon. Journal of Geophysical Research 115, C08018, http://dx.doi.org/10.1029/2009JC005731.

Bailey, K.M., Abookire, A., Duffy-Anderson, J.T., 2008. Ocean transport paths for the early life stages of offshore-spawning flatfishes: a case study in the Gulf of Alaska. Fish and Fisheries 9, 44–66.

Blood, D.M., Matarese, A.C., 2010. Larval development and identification of the genus *Triglops* (Scorpaeniformes: Cottidae). NOAA Prof. Paper, 10. NMFS. 49 pp.

Blood, D.M., Matarese, A.C., Yoklavich, 1994. Embryonic development of walleye pollock, *Theragra chalcogramma*, from Shelikof Strait, Gulf of Alaska. Fishery Bulletin 97, 207–222.

Bowering, W.R., Nedreaas, K.H., 2000. A comparison of Greenland halibut (*Reinhardtius hippoglossoides* (Walbaum)) fisheries and distribution in the northwest and northeast Atlantic. Sarsia 85, 61–76.

Bulatov, O.A., 1983. Distribution of eggs and larvae of Greenland halibut *Reinhardtius hippoglossoides* (Pleuronectidae) in the eastern Bering Sea. Journal of Ichthyology 23, 157–159.

Carter, G.S., Gregg, M.C., 2002. Intense, variable mixing near the head of Monterey submarine canyon. American Meteorological Society 32, 3145–3165.

Curchitser, E.N., Haidvogel, D.B., Hermann, A.J., Dobbins, E.L., Powell, T.M., Kaplan, A., 2005. Multi-scale modeling of the North Pacific Ocean: assessment and analysis of simulated basin-scale variability (1996–2003). Journal of Geophysical Research 110, http://dx.doi.org/10.1029/2005JC002902.

Di Lorenzo, E., Schneider, N., Cobb, K.M., Franks, P.J.S., Chhak, K., Miller, A.J., McWilliams, J.C., Bograd, S.J., Arango, H., Curchitser, E., Powell, T.M., Rivière, P., 2008. North Pacific gyre oscillation links ocean climate and ecosystem change. Geophysical Research Letters 35 (L08607), http://dx.doi.org/10.1029/2007GL032838.

Duffy-Anderson, J.T., Blood, D.M., Mier, K.L., 2011. Stage-specific vertical distribution of Alaska plaice (*Pleuronectes quadrituberculatus*) eggs in the eastern Bering Sea. Fishery Bulletin 109, 162–169.

Fahay, M.P., 2007. Pleuronectidae. In: Fahay, M.P. (Ed.), Early Stages of Fishes in the Western North Atlantic Ocean, Vol. II. Northwest Atlantic Fisheries Organization, Dartmouth, Nova Scotia, Canada, pp. 1536–1549. 1696 pp.

Fiechter, J., Moore, A.M., Edwards, C.A., Bruland, K.W., Di Lorenzo, E., Lewis, C.V.W., Powell, T.M., Curchitser, E., Hedstrom, K., 2009. Modeling iron limitation of primary production in the coastal Gulf of Alaska. Deep Sea Research Part II: Topical Studies in Oceanography 56 (24), 2503–2519.

Grebmeier, J.M., Overland, J.E., Moore, S.E., Farley, E.V., Carmack, E.C., Cooper, L.W., Frey, K.E., Helle, J.H., McLaughlin, F.A., McNutt, S.L., 2006. A major ecosystem shift in the northern Bering Sea. Science 311 (5766), 1461–1464.

Gunderson, D.R., Ellis, I.E., 1986. Development of a plumb staff beam trawl for sampling demersal fauna. Fisheries Research 4, 35–41.

Haidvogel, D.B., Arango, H.G., Hedstrom, K., Beckmann, A., Malanotte-Rizzoli, P., Shchepetkin, A.F., 2000. Model evaluation experiments in the North Atlantic Basin: simulations in nonlinear terrain-following coordinates. Dynamics of Atmospheres and Oceans 32, 239–281.

Hermann, A.J., Hinckley, S., Dobbins, E.L., Haidvogel, D.B., Bond, N.A., Mordy, C., Kachel, N., Stabeno, P.J., 2009. Quantifying cross-shelf and vertical nutrient flux in the Gulf of Alaska with a spatially nested, coupled biophysical model. Deep Sea Research Part II: Topical Studies in Oceanography, http://dx.doi.org/10.1016/j.dsr2.2009.02.008.

Hickey, B.M., Banas, N.S., 2008. Why is the northern end of the California Current system so productive? Oceanography 21, 90–107.

Hoff, G.R., 2010. Identification of skate nursery habitat in the eastern Bering Sea. Marine Ecology Progress Series 403, 243–254.

Ianelli, J.N., Wilderbuer, T.K., Nichol, D., 2011. Assessment of Greenland turbot in the eastern Bering Sea and Aleutian Islands. Bering Sea and Aleutian Islands Stock Assessment and Fishery Evaluation report. North Pacific Fishery Management Council, Anchorage, AK. 696 pp.

Iles, T.D., Sinclair, M., 1982. Atlantic herring: stock discreteness and abundance. Science 215 (4533), 627–633.

Jensen, A., 1935. The Greenland halibut (*Reinhardtius hippoglossoides*), its development and migration. Kongelige Danske Videnskabernes Selskabs. Biologiske Skrifter 9, 1–32.

Kämpf, J., 2005. Cascading-driven upwelling in a submarine canyon at high latitudes. Journal of Geophysical Research 110, C02007, http://dx.doi.org/10.1029/2004JC002554.

Kendall Jr., A.W., Ahlstrom, E.H., Moser, H.G., 1984. Early life history stages and their characters. Am. Soc. Ichthyol. Herpetol In: Moser, H.G., et al. (Ed.), Ontogeny and Systematics of Fishes. Spec. Publ., 1. Allen Press, Lawrence, KS, pp. 11–22. 652 pp.

Kunze, E., Rosenfeld, L.K., Carter, G.S., Gregg, M.C., 2002. Internal waves in Monterey Submarine Canyon. Journal of Physical Oceanography 32, 1890–1913.

Love, M.S., Yoklavich, M., Thorsteinson, L., 2002. The Rockfishes of the Northeast Pacific. University of California Press, Los Angeles, CA. 390 pp.

Magnusson, J.V.M.S., 1977. Notes on the eggs and larvae of Greenland halibut at Iceland. ICES C.M. Doc., No. F: 47.

Matarese, A.C., Kendall Jr., A.W., Blood, D.M., Vinter, B.M., 1989. Laboratory guide to early life history stages of Northeast Pacific fishes. NOAA Tech. Rep. NMFS 80. 652 pp.

Matarese, A.C., Blood, D.M., Picquelle, S.J., Benson, J.L., 2003. Atlas of abundance and distribution patterns of ichthyoplankton from the Northeast Pacific Ocean and Bering Sea ecosystems based on research conducted by the Alaska Fisheries Science Center (1972–1996). NOAA Prof. Pap. NMFS 1. 281 pp.

Mikawa, M., 1963. Ecology of the lesser halibut *Reinhardtius hippoglossoides matsuurae*. Bulletin of Tohoku Regional Fisheries Research Laboratory 23, 1–43.

Minami, T., Tanaka, M., 1992. Life history cycles in flatfish from the northwestern Pacific, with particular reference to their early life histories. Netherlands Journal of Sea Research 29, 35–48.

Moser, H.G., 1996. Introduction. In: Moser, H.G. (Ed.), The Early Life Stages of Fishes in the California Current Region: Calif. Coop. Oceanic Fish. Invest. Atlas No., 33, pp. 1–50. 1505 pp.

Normark, W.R., Carlson, P.R., 2003. Giant submarine canyons: is size any clue to their importance in the rock record? In: Chan, M.A., Archer, A.W. (Eds.), Extreme Depositional Environments: Mega End Members in Geologic Time. The Geological Society of America, Inc., Boulder, CO. 281 pp.

Pertseva-Ostroumova, T.A., 1961. The reproduction and development of far-eastern flounders. Tr. Inst. Okeanol. Akad. Nauk SSSR. 484 pp. [In Russian; Eng. transl. avail. Fish. Res. Bd. Can., Pac. Biol. Stn., Nanaimo, B.C., Canada V9R 5K6, Transl. Ser. 856, 1967.].

Schmidt, J., 1904. On pelagic post-larval halibut *Hippoglossus vulgarus* Flem. and *H. hippoglossoides* (Walbaum). Meddr. Kommn Havunders. Ser. Fiskei 1 (3) 12 pp.

Shchepetkin, A.F., McWilliams, J.C., 2005. The regional oceanic modeling system (ROMS): a split-explicit, free-surface, topography-following-coordinate oceanic model. Ocean Modelling 9 706 (4), 347–404.

Sigler, M.F., Renner, M., Danielson, S., Eisner, L.B., Lauth, R., Kuletz, K.J., Logerwell, L.A., Hunt Jr., G.L., 2011. Fluxes, fins and feathers: relationships among the Bering, Chukchi, and Beaufort Seas in a time of climate change. Oceanography 24 (3), 112–127.

Sinclair, E.H., Stabeno, P.J., 2002. Mesopelagic nekton and associated physics of the southeastern Bering Sea. Deep Sea Research Part II: Topical Studies in Oceanography 49 (26), 6127–6145.

Sohn, D., Ciannelli, L., Duffy-Anderson, J.T., 2010. Distribution and drift pathways of Greenland halibut (*Reinhardtius hippoglossoides*) during early life stages in the eastern Bering Sea and Aleutian Islands. Fisheries Oceanography 19 (5), 339–353.

Stabeno, P.J., Schumacher, J.D., Ohtani, K., 1999. The physical oceanography of the Bering Sea. In: Loughlin, T., Ohtani, K. (Eds.), University of Alaska Sea Grant, Fairbanks, AK, pp. 1–28. 825 pp.

Stabeno, P.J., Kachel, N.B., Moore, S., Napp, J., Sigler, M., Yamaguchi, A., Zerbini, A., 2012. Comparison of warm and cold years on the southeastern Bering Sea shelf and some implications for the ecosystem. Deep Sea Research II 65–70, 31–45.

Stene, A., Gundersen, A.C., Albert, O.T., Nedreaas, K.H., Solemdal, P., 1999. Early development of northeast arctic Greenland halibut (*Reinhardtius hippoglossoides*). Journal of Northwest Atlantic Fishery Science 25, 171–177.

St-Pierre, G., 1984. Spawning location and season for Pacific halibut. International Pacific Halibut Commission Science Reports 70.

Tsukamoto, Y., Ueno, Y., Minami, T., Okiyama, M., 1995. Transforming specimens of two righteye flounders, *Atheresthes evermanni* and *Reinhardtius hippoglossoides*. Japan Journal of Ichthyology 41, 469–473.

Wiebe, P.H., Burt, K.H., Boyd, S.H., Morton, A.W., 1976. A multiple opening/closing net and environmental sensing system for sampling zooplankton. Journal of Marine Research 34, 313–326.